Legends to figures:

Figure 1: The three components of a typical nanotheranostic system: the carrier, the imaging label and the bioactive molecule

Figure 2: Passive and active targeting strategies for nanotheranostics to reach the tumor

Figure 3: A) Stem cells were loaded either with PFOB or PFCE emulsions and injected into mouse thigh skeletal right or left muscle. B-C) ^{19}F MR imaging at 11.7 T (4 min scan time) by selecting the appropriate RF excitation frequencies for PFOB (B) and for PFCE (C). D) Overlay of B and C images onto a conventional ^{1}H anatomical image reveals PFOB and PFCE labelled cells localized to the left and right leg, respectively [37].

Figure 4: Top) T_2-weighted fast-spin echo images in the tumor (dashed circle) before injection and 2 and 48 hours later. Bottom) Tumor growth for 25 days proving the antitumor activity of aptamer conjugated nanoparticles loaded with doxorubicin, which is represented on the right side [66].

Figure 5: Top) Photographs of the subcutaneous tumor twelve days after treatment, which consisted in systemic administration of empty or paclitaxel loaded droplets followed by focused ultrasound application Bottom) Evolution of the tumor size for pancreatic cancer bearing mice treated with either empty (open symbols) or PTX-loaded PFCE nanodroplets (closed symbols). ^{19}F MR image superimposed with anatomical ^{1}H MR image of a coronal slice of the mouse after 4 systemical injections (every 2 hours) of PFCE nanodroplets [67].

Figure 6: a),d)Raw signal intensity maps show axial views of the rat bearing tumor with a central heating catheter at t=0min (a) and t=45min (d) after dox loaded liposomes injection. b) and e) T1 converted maps from a) and d) respectively. c) Calculated Dox concentration from images b and e. f) Enlarged image of c) showing the heterogenehity in drug delivery within the tumor. g), h)Linear correlation between HPLC and histological respectively with relaxivity measurements validated [Dox] measurements. i) Overlay of g and h showing the precision and accuracy of MRI for measuring Dox at low concentrations [74].

Figure 1

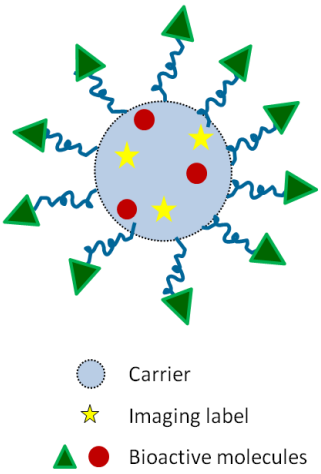

Figure 2

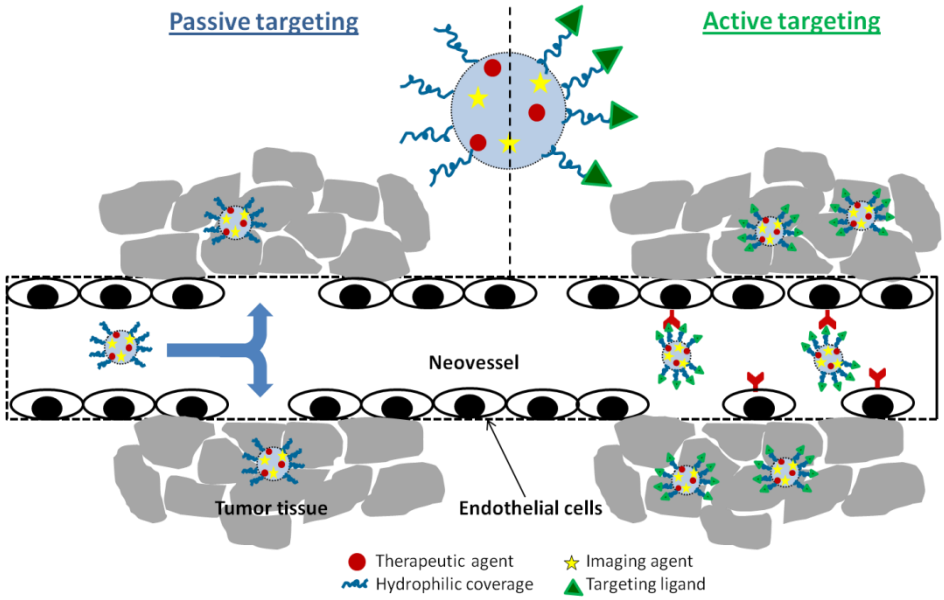
Passive targeting
Active targeting
Neovessel
Tumor tissue
Endothelial cells
Therapeutic agent
Hydrophilic coverage
Imaging agent
Targeting ligand

Figure 3

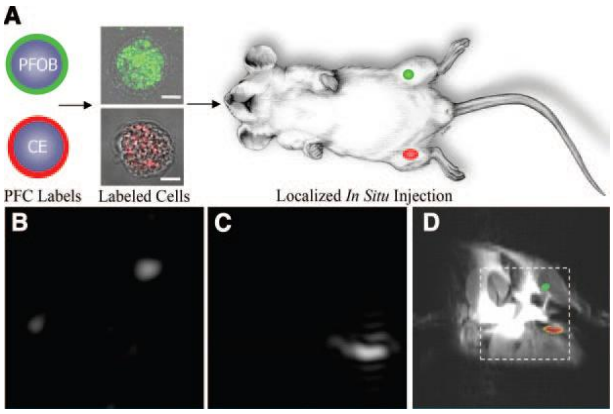
A
PFOB
CE
PFC Labels
Labeled Cells
Localized *In Situ* Injection
B
C
D

Figure 4

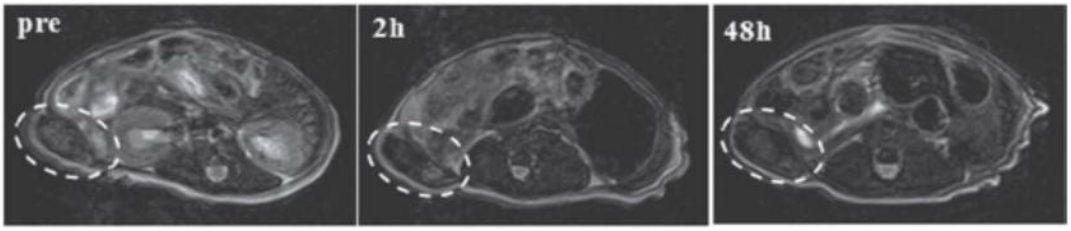
pre
2h
48h

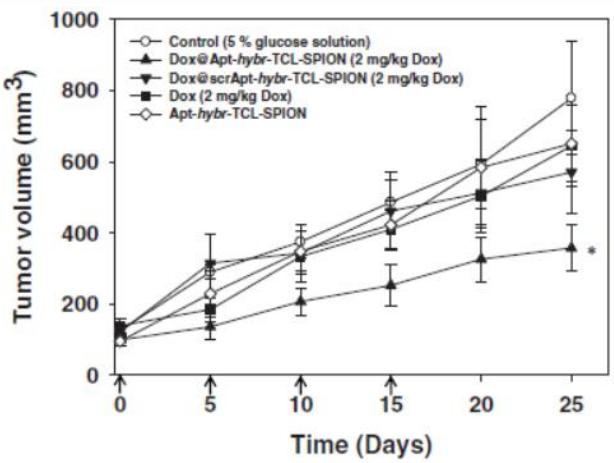
Control (5 % glucose solution)
Dox@Apt-hybr-TCL-SPION (2 mg/kg Dox)
Dox@scrApt-hybr-TCL-SPION (2 mg/kg Dox)
Dox (2 mg/kg Dox)
Apt-hybr-TCL-SPION
Tumor volume (mm3)
Time (Days)
0
200
400
600
800
1000
0
5
10
15
20
25
*

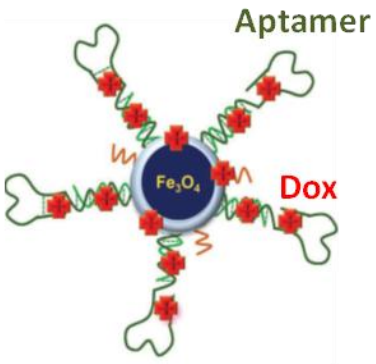
Aptamer
Fe3O4
Dox

Figure 5

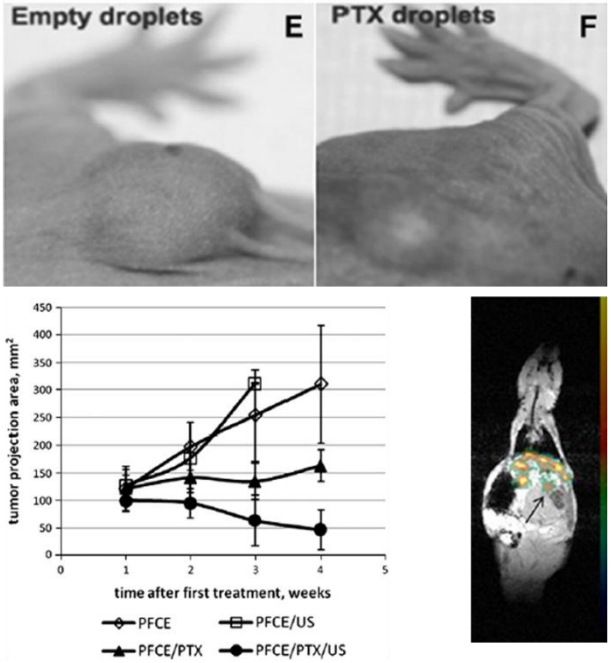
Empty droplets
E
PTX droplets
F
tumor projection area, mm²
time after first treatment, weeks
PFCE
PFCE/US
PFCE/PTX
PFCE/PTX/US

Figure 6

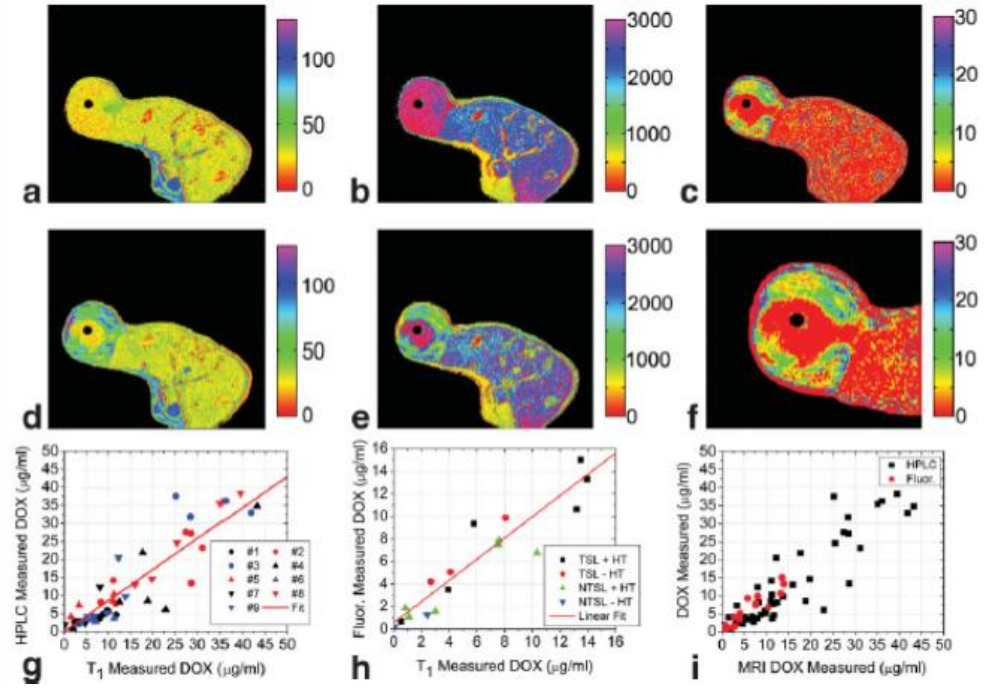
a
100
50
0
b
3000
2000
1000
0
c
30
20
10
0
d
100
50
0
e
3000
2000
1000
0
f
30
20
10
0
HPLC Measured DOX (μg/ml)
#1
#2
#3
#4
#5
#6
#7
#8
#9
Fit
g
T1 Measured DOX (μg/ml)
Fluor. Measured DOX (μg/ml)
TSL + HT
TSL - HT
NTSL + HT
NTSL - HT
Linear Fit
h
T1 Measured DOX (μg/ml)
DOX Measured (μg/ml)
HPLC
Fluor.
i
MRI DOX Measured (μg/ml)